ADVANCES IN THE SOIL HYDRAULIC PROPERTIES MEASUREMENTS WITH THE TENSION INFILTROMETRY TECHNIQUE

D. Moret-Fernández [1*], B. Latorre [1], C. González-Cebollada [2] and C. Peña [1]

[1]Departamento de Suelo y Agua Estación Experimental de Aula Dei, Consejo Superior de Investigaciones Científicas (CSIC), PO Box 202, 50080 Zaragoza, Spain. e-mail: david@eead.csic.es, http://www.eead.csic.es
[2]Área de Mecánica de Fluidos. Escuela Politécnica Superior de Huesca - Universidad de Zaragoza. Carretera de Cuarte s/n. 22071, Huesca, España.

RESUMEN. Esta comunicación presenta varios avances realizados en la técnica de infiltrometría de tensión. (i) Nuevas bases de disco que permiten medidas de infiltración sin utilizar arena de contacto (disco de base adaptable) o sobre cobertura vegetal (base con forma de sombrero). (ii) Estimación de la conductividad hidráulica (K) y sorptividad (S) del suelo a partir de la solución numérica de la ecuación cuasi-analítica de la curva de infiltración acumulada 3D (NSQE). Los resultados muestran que los prototipos presentados permiten medir de forma satisfactoria la curva de infiltración acumulada de agua en el suelo. Paralelamente, el método NSQE aplicado sobre 400 medidas de infiltración ha resultado ser robusto y ofrece estimaciones más precisas de K y S.

ABSTRACT. This work presents several advances made on the infiltrometry technique. (i) A new disc base that allows infiltration measurements without contact sand layer (malleable disc base) or on plants cover (hat infiltrometer). (ii) Estimate of the soil hydraulic conductivity (K) and sorptivity (S) from the numerical solution of the quasi-analytical form of the 3 D cumulative infiltration curve (NSQE). After analysing the different disc designs and the accuracy of the NSQE method on 400 infiltration measurements, the results show that the new prototypes are viable and the NSQE method is robust enough and allows better estimates of K and S.

1.- Introduction

Infiltration-based methods are recognised as valuable tools for studying hydraulic and transport soil properties. Over the last two decades tension disc infiltrometers (Perroux and White, 1988) have become very popular devices for in situ estimates of soil surface hydraulic properties such as saturated and unsaturated hydraulic conductivity (Angulo-Jaramillo et al., 2000). An important advantage of this technique is that it is a relatively rapid and portable method, which allows exploration of the dependence of hydraulic properties on soil structure.

Typically, this instrument consists of three parts made of Plexiglass: a base disc covered by a nylon cloth, a graduated reservoir that provides the water-supply, and a bubble tower with a moveable air-entry tube that imposes the pressure head of the water at the cloth base (Angulo-Jaramillo et al., 2000) (Fig. 1). The soil hydraulic properties are commonly estimated from the analysis of the cumulative infiltration curve measured from the water-supply reservoir.

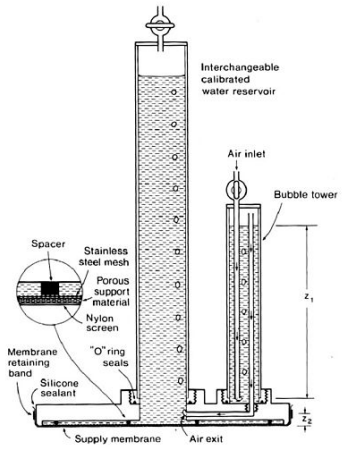

Fig.1. Disc infiltrometer diagram

The base disc: The diameter of the disc base can range from the 25 cm originally proposed by Perroux and White (1988) to the 3.2 cm used by Madsen and Chandler (2007). Correct measurements of the infiltration curve require the membrane of the disc base to be completely in contact with the soil surface. To achieve this contact, Perroux and White (1988) recommended trimming any vegetation within the sample to ground level and covering the soil with a material that had a greater hydraulic conductivity than the soil. According to Reynolds (2006), the contact sand layer introduces an offset between the pressure head set on the bubble tower and the pressure head applied to the soil surface, which has varying impacts on relationships describing near-saturated hydraulic properties. The amount of overestimate and underestimate should be corrected using a form of Darcy's law to prevent the introduction of systematic biases in infiltration results (Reynolds, 2006). Minasny and McBratney (2000) concluded that contact sand was recommended because, otherwise, the poor contact between the disc base and the soil surface makes the

absolute rate of infiltration considerably lower. This makes that field measurements with conventional disc infiltrometer were more tedious and time consuming.

The rigid disc base used by the disc infiltrometer prevents infiltration measurements on abrupt surfaces or soils covered with plants or crop residues. This problem was partially solved by UGT (Müncheberg, Germany), who developed a tension infiltrometer where the disc base was replaced by an acrylic hood. The hood is placed open side down onto the soil, within a retaining ring inserted into the soil, and the water-filled hood is directly in contact to the soil surface. Although this new system allows infiltration measurements on covered soils, the characteristics of this design introduces two limitations during the infiltration measurements: (i) the retaining ring used to close the hood, which is slightly inserted into the soil, may create preferential infiltration channels that distort the infiltration measurements; and (ii) the slow hood water-filling during the firsts infiltration steps prevents employing the transient water flow method to estimate the soil hydraulic properties. In this case, the hydraulic properties should be measured using the steady-state flow method, which has proven to be more time consuming.

Estimate of k and s: Various techniques are so far available for inferring hydraulic properties from the measured cumulative infiltration curves: the steady-state and the transient water flow methods. Compared to the standard the steady-state water flow method (Ankeny et al., 1991), the transient water flow procedure, that requires shorter experiments, involves smaller sampled soil volumes and consequently more homogeneous and initial water uniformity (Angulo-Jaramillo et al., 2000). Several simple expressions have been developed to estimate the soil hydraulic parameters from the transient water flow (Warrick and Lomen, 1976; Warrick, 1992, Zhang, 1997). However, based on the quasi-exact analytical form of the three-dimensional cumulative infiltration curve from the disc infiltrometer developed by Haverkamp et al. (1994), these same authors proposed a physically based simplified expression, valid for short to medium time, which allowed easy calculation of K and S from the transient water flow. Vandervaere et al. (2000) compared several methods to analyze the simplified Haverkamp et al. (1994) equation and concluded that the linear fitting technique consisting of a differentiation of the cumulative infiltration data with respect to the square root of time (DL) allowed the best estimations of soil hydraulic properties when contact sand layer was used. However, the validity of the DL method, which is only applicable for short to medium time, is questioned when infiltration is controlled by capillary forces (Angulo-Jaramillo et al., 2000). On the other hand, the discontinuous bubbling in the water-supply reservoir, which makes a kind of stair-shaped cumulative infiltration curves (Moret-Fernández et al. 2012a), can results in highly "noised" differentiated regression lines that prevents accurate estimations of K and S (Moret-Fernández et al. 2012b).

The objective of this paper is to present new advances applied to the tension infiltrometry technique to estimate the soil hydraulic properties. These advances are focused on: (i) a new procedure to calculate K and S by numerically solving the quasi-exact analytical of the Haverkamp et al. (1994) form for the unsaturated cumulative infiltration curves, which has been subsequently tested on 400 cumulative infiltration curves recorded under different soils and structural conditions; and (ii) alternative disc bases that allows complete contact between the infiltrometer base and the soil surface without using a contact sand layer (maleable disc base) and on soil surfaces with plants covering (hat infiltrometer).

2.- Material and methods

2.1.- Estimate of K and S

Haverkamp et al. (1994) found that the three-dimensional infiltration, I_{3D}, equation for unsaturated conditions yields

$$\frac{2(K_0-K_n)^2}{S_0^2}t=\frac{2}{1-\beta}\frac{K_0-K_n}{S_0^2}\cdot\left\{I_{3D}-K_nt-\left[\gamma S_0^2/R_D(\theta_0-\theta_n)\right]\right\}-\frac{1}{1-\beta}\cdot\ln\left\{\left\{\exp\left[2\beta(K_0-K_n)/S_0^2\right]\left[I_{3D}-K_nt-\left(\gamma S_0^2/R_D(\theta_0-\theta_n)\right)\right]+\beta-1\right\}^{(\beta)^{-1}}\right\} \quad (1)$$

where R_D (m) is the radius of the disc, θ_0 and θ_n are the final and initial volumetric water content (m^3 m^{-3}), respectively, K_0 and K_n are the hydraulic conductivity values corresponding to θ_0 and θ_n, S_0 is the sorptivity (m $s^{-0.5}$) for θ_0, γ is the proportionality constant (approximated to 0.75; Angulo-Jaramillo et al., 2000), and β is a shape constant constrained to $0 < \beta < 1$ (average value of 0.6; Angulo-Jaramillo et al., 2000). This equation is valid for the entire time range from $t = 0$ to $t = \infty$. Due to the relative complexity of the three-dimensional infiltration equation, no analytical solution is available. In order to obtain the desired infiltration curve, $I(t)$, Eq. (1) must be numerically solved for each measurement time value. Assuming a given time and known soil parameters, Eq. (1) can be grouped as a function depending on the infiltration.

$$f(I)=0 \quad (2)$$

Determining the value that satisfies $I(t)$ in Eq. (1) is equivalent to finding the root or zero of function $f(I)$. For this purpose, the bisection method has been used. The procedure begins defining an interval $[I_1, I_2]$ where $f(I_1)$ and $f(I_2)$ have opposite signs. If $f(I)$ is continuous on the interval, the intermediate value theorem guarantees the existence of at least one root between I_1 and I_2. At each step, the interval is divided in two by computing its midpoint $I_3=(I_1+I_2)/2$ and the corresponding value of the function $f(I_3)$ for that value.

Depending on the sign of $f(I_3)$, the subinterval containing the root is selected and used in the next step.

$$\text{If} \quad sign[f(I_3)] = sign[f(I_1)] \quad I_1 = I_3 \qquad (3)$$
$$\text{Otherwise,} \quad I_2 = I_3$$

Following this procedure, the solution is iteratively approximated reducing the size of the interval until is sufficiently small. Considering that K and S can vary by several orders of magnitude, the minimum size of the interval was estimated to preserve the relative accuracy of the results

$$I_2 - I_1 > \varepsilon \frac{I_1 + I_2}{2} \qquad (4)$$

where the following tolerance value has been used: ε = 0.001. The initial interval lower bound, I_1, was set to zero and the upper limit was chosen in each case to a value much larger than the maximum expected infiltration.

When considering extreme values of *K* or *S*, the nonlinear character of Eq. (1) leads to high numerical errors related to the computer arithmetic precision, typically performed using 64 bits. To overcome this problem, the arbitrary-precision library GNU Multiple Precision Arithmetic Library (GMP) has been used with 128 precision bits.

Soil hydraulic properties are estimated fitting the numerical solution of Eq. 1 to the measured cumulative infiltration data. This process consists of an optimization to minimize the difference between the theoretical and experimental infiltration curves, where a root mean squared error (RMSE) estimator was considered.

The simple and robust brute force (BF) method has been used to calculate all possible solutions of the hydraulic properties. Even this technique requires considerable computation effort, BF was applied as a reference method providing detailed information on the error distribution to guide the future use of more efficient optimization methods.

In each optimization, a fixed parameter interval was explored

$$K_0 \in [10^{-6},\ 10] \ \text{mm/s} \qquad (5)$$
$$S_0 \in [10^{-2},\ 10] \ \text{mm/s}^{1/2}$$

using a logarithmically spaced grid of 200×200 points and then selecting the best (K_0, S_0) pair according to the minimum RMSE found.

Correct infiltration measurement requires in some situations the use of contact sand layer, whose influence on the cumulative infiltration curve should be removed. For this purpose, the experimental data was repeatedly fitted to Eq. (1) considering different (I, t) shifts along the measured infiltration curve. The best fit to the infiltration model, which does not include the sand effect, defines the part of the curve that must be discarded to remove the influence of the contact layer.

Fitting Eq. (1) to a measured infiltration curve allows determination of soil hydraulic properties but does not provide information about the uncertainty of these values. Although, in practice, there are several sources of uncertainty, this section focuses on the theoretical limitations of the infiltration model. Optimization interval (9) was considered computing, for each explored point (K_0, S_0), a confidence interval based on the near RMSE distribution, typically parabolic, associated to the curve auto-fitting. The error increase that defines the size of the confidence interval has been estimated based on the typical precision of the cumulative infiltration measurement (1/16 mm), determining the ability to distinguish between two infiltration curves.

Numerical results show that the uncertainty associated to the model fitting depends strongly on the considered infiltration time, due to the increasing shape of the cumulative infiltration curve. For this reason, the study has been oriented to calculate the minimum measurement time to obtain a fixed precision in the parameters estimation for each (K_0, S_0) result.

Haverkamp et al. (1994) established that, for short to medium time and assuming $K_n \to 0$, the 3D cumulative infiltration curve could be simplified to

$$I_{3D} = C_1\sqrt{t} + C_2 t \qquad (6)$$

where

$$C_1 = S_0$$
$$C_2 = \frac{2-\beta}{3}K_0 + \frac{\gamma S_0^2}{R_D(\theta_n - \theta_0)} \qquad (7)$$

Vandervaere et al. (2000) proposed to calculate K and S by a linear fitting technique ["differentiated linearization" (DL)] that consists in differentiating the cumulative infiltration curve (Eq. 2) with respect to the square root of time,

$$\frac{dI}{d\sqrt{t}} = C_1 + 2C_2\sqrt{t} \qquad (8)$$

and next plotting the $\frac{dI}{d\sqrt{t}}$ term as a function of $\sqrt{t}$. In this model, C_1 is the intercept and C_2 the slope of the corresponding regression lines. According to these authors, the DL technique was the only method that allowed visual monitoring the validity of Eq. (2) when contact sand layer was used. This technique was good for revealing and eliminating, at the beginning of experiments, the influence of the sand contact layer, which may have negative effects on parameter estimations when not taken into account.

The NSQE model was tested with infiltration

measurements performed in semiarid dry lands of the central Ebro Basin (north-eastern Spain). The average annual precipitation of the experimental fields ranges between 313 and 350 mm. The experimental fields were located in the municipalities of Peñaflor, Codo, Belchite, Leciñena, Sariñena and Bujaraloz. The lithology of the fields is non-gypseous alternating with gypseous areas. The traditional land use in the region is an agro-pastoral system involving rainfed agriculture and extensive sheep grazing. The cropping system in these semi-arid dry lands is a traditional cereal–fallow rotation, which involves a long fallow period of 16–18 months, running from June–July to November–December of the following year.

Five different contrasted soil managements were considered: ungrazed (NG) and grazed (GR) uncultivated lands (N), and conventional (CT), reduce (RT) and no-tillage (NT) treatments of cultivated soil. The NG and GR treatments were located on uncultivated soils at Leciñena, Belchite, Codo and Sariñena municipalities (Moret-Fernández et al. 2011). Agricultural fields with CT, RT and NT treatments were located in Peñaflor (Moret and Arrúe, 2007) and Bujaraloz (Moret-Fernández et al., 2013). The CT and RT treatment used a mouldboard and chisel ploughing of fallow plots in late winter or early spring, respectively. NT used exclusively herbicides (glyphosate) for weed control throughout the fallow season. Three different soil structural conditions were considered in cultivated soils: freshly moldboard tilled (MB), cropped (C), and fallowed (F) soils. All measurements were conducted on nearly level areas (slope 0–2%) between February 2000 and April 2001, and February 2009 and October 2010.

The soil hydraulic properties were measured with a Perroux and White (1988) model tension disc infiltrometer (DI). Three different diameter discs were tested: 60 (D_{60}), 100 (D_{100}) and 250 (D_{250}) mm external diameters, respectively. Two different base discs were used: (i) a conventional disc (C_{DB}) and a malleable base disc (M_{DB}), (see section 2.2). Infiltration measurements were taken on areas cleared of large clods and crop residue. These included infiltration measurements on the soil surface crust and on the 1–10 cm depth soil layer, after removing the surface crust. For the conventional disc (C_{DB}) a thin layer (< 1 cm thick) of commercial sand (80–160 μm grain size), with the same diameter as the disc base, was poured onto the soil surface. The M_{DB} disc was directly placed on the soil surface. A total of 400 cumulative infiltration curves measured with the three different disc bases were compared: 43, 265 and 93 infiltration curves measured with the D_{60} D_{100} D_{250} discs, respectively. All measurements were performed at soil saturation conditions, except the D_{250} that included 74 infiltration curves at -14 cm of soil tension. The cumulative water infiltration was measured from the drop in water level of the reservoir tower. Water levels in the D_{250} infiltrometer were automatically monitored with the TDR technique (Moret et al., 2004). D_{60} and D_{100} infiltrometer monitored water level drops with ±0.5 psi differential pressure transducer (PT) (Microswitch, Honeywell) (Casey and Derby, 2002). The scanning time interval was 5 and 10 seconds for the PTs and TDR water level monitoring techniques, respectively. Infiltration measurements lasted between 8 and 15 min for soil saturated conditions and 30 min for -14 cm soil tensions infiltration measurement. At the end of infiltration, a wet soil sample was also taken to estimate the final volumetric water content.

Measured infiltration data were used to check the accuracy and sensitivity of the NSQE method to estimate *S* and *K*. In a first analysis, the influence of the contact sand layer on the NSQE applicability was studied. The results were compared to those obtained with the DL method. Next, the *S* and *K* estimated with the NSQE method for all measured infiltration curves were compared with the corresponding values estimated with the DL procedure (when able). To prevent subjective decisions when using the DL method, the following considerations were established: (i) the time differential (dt) chosen for the DL regression lines (Eq. 5) was in all cases ≤ 10 s (higher dt values involves smoothing the DL regression lines); (ii) except for the firsts infiltration seconds corresponding to the contact sand layer, no experimental points from the $\frac{dI}{d\sqrt{t}}$ vs. $\sqrt{t}$ relationship (Eq. 5) were removed; (iii) total time considered in the DL method was < 150 s. On the other hand, comparison between DL and NSQE models involved the following conditions: (i) no negative K or S results were considered; and (ii) $\frac{dI}{d\sqrt{t}}$ vs. $\sqrt{t}$ relationships with regression coefficient (R^2) < 0.15 were omitted. The selected DL regression lines (R^2 > 0.15) were grouped in two sets: regression lines with R^2 between 0.15 and 0.60, and DL lines with $R^2 > 0.60$.

2.2.- Disc bases

Two disc bases are presented: malleable disc base and the hat infitrometer.

Malleable disc base: This base (M_{DB}) consists on 10-cm-diameter disc, with an inner conical wall that allows the bubbles to be driven from the disc base to the reservoir tower and a metallic grid (with 1-cm square holes) glued at the base, covered with malleable nylon cloth of 20-μm mesh (air entry value of about _7.5 kPa) filled with 100 g of coarse sand (1- to 1.5-mm grain size) (Fig. 2) (approximately 0.5-cm-thick layer). This design allows the loosened nylon cloth to adapt to a relatively smooth area when the infiltrometer is placed on the soil surface. The M_{DB} was compared to a same geometry conventional disc (CDB), in which the base was covered with a tightened nylon cloth and used contact sand layer between the soil surface and the base disc.

The two disc bases were compared in a series of field experiments on structured soils under different forms of tillage management. The site is located at the dryland research farm of the Estación Experimental de Aula Dei in the province of Zaragoza (Moret and Arrúe, 2007). The

climate is semiarid and the soil is a loam (fine-loamy, mixed thermic Xerollic Calciorth id) according to the United States Department of Agriculture soil classification (Soil Survey Staff, 1975).

Fig 2. Malleable disc base

Three different tillage treatments were compared: conventional tillage (CT), reduced tillage (RT) and notillage (NT). The tillage treatments were arranged in a complete block design, with basic basic plots of was 33.5 x 10 m. One infiltration measurement with M_{DB} and C_{DB} discs was performed per plot (3 replications per tillage management and type of disc base). The soil dry bulk density (ρ_b) was determined using the core method (50mm diameter x 50mm high cores) height. Infiltration measurements were taken on areas cleared of surface crust, large clods and crop residue. For C_{DB} a thin layer (<1 cm thick) of commercial sand (80- to 160-mm grain size and an air entry value between -1 and -1.5 kPa), with the same diameter as the disc base, was poured onto the soil surface. The M_{DB} was directly placed on the soil surface. The cumulative water infiltration was measured from the drop in water level of the reservoir tower. The scanning time interval for the PTs was 5 s, and the infiltration measurements lasted up to 8–10 min in total. The soil surface after infiltration measurements and the cumulative infiltration curves measured with both disc infilrometers were analysed. Finally, the S and K values calculated with the C_{DB} using the Vandervere et al. (2000) (section 2.1) were compared to that estimated with the M_{DB} plates.

Hat infiltrometer: The hat infiltrometer (HI) consists of a hat-shape base jointed at the top to a water-supply reservoir and a bubble tower to impose a negative pressure head at the hat base (Fig. 3a). The hat base is a cylindrical acrylic tube (10 cm internal diameter –i.d-; 10 cm height) jointed at the base to a metallic flat ring (3 mm thickness and 10 and 15 cm internal and external diameter, respectively) and closed at top by an acrylic lid. Three T-shape iron arms are equidistantly welded on the metallic ring (Fig. 3b). The water reservoir consists of a 5 cm i.d. and 55 cm high acrylic tube, which is connected to the hat through vertical acrylic tube assembled to a water flow ball (Fig. 3a). This acrylic tube (3.4 cm i.d.), which vertically crosses the hat, rests at 1.5 cm on the soil surface. A tube 8 mm i.d. silicone pipe connects the top of the water reservoir to the top of the hat (Fig. 3a). The base of the hat is connected to the bubble tower by a 3 mm i.d. plastic pipe. To check the pressure head on the soil surface a water manometer was inserted at the top of the hat. A ±0.5 psi differential pressure transducer (PT) (Microswitch, Honeywell), connected to a datalogger (CR1000, Campbell Scientist Inc.), was installed at the bottom of the water-supply reservoir (Casey and Derby, 2002). The hat base is closed at the bottom by compressing the HI base against the soil surface. To this end, a plasticine ring placed below the metallic ring plus a T-shape sticks system is used (Fig. 3b).

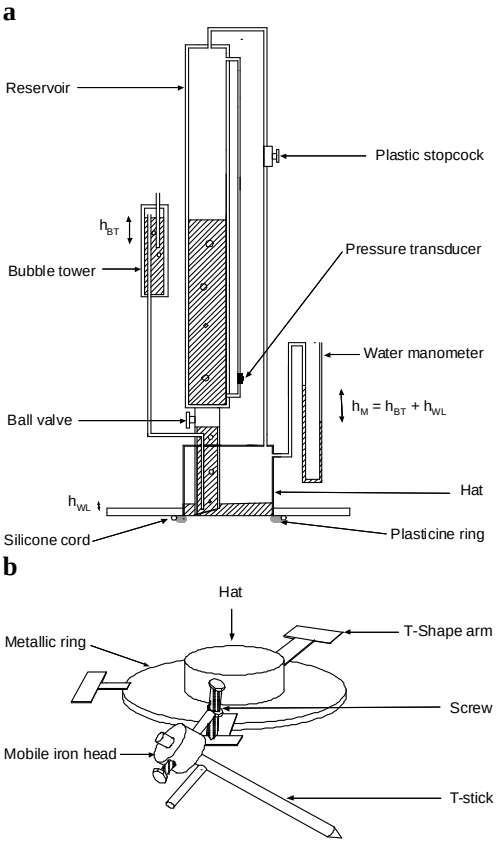

Fig. 3. Malleable disc base (a) and hat base (b)

Hat infiltrometer setting up needed the following steps. Firstly, the hat plus plasticine ring (11 cm i.d. and 2 cm thickness) are placed on the soil surface to be measured. In order to minimize the soil surface disturbance during the hat water-filled, a 10 cm diameter cloth is placed on the soil surface within the hat. The three T-shape sticks are equidistantly and obliquely hammered into the soil in such a way that the sticks ends rest in front of the hat ring iron arms (Fig. 3b). A mobile iron head, which incorporates a screw (8 cm length and 0.8 cm diameter), is inserted at the end of the T-shape stick (Fig. 3b). The mobile iron head is blocked in a way that the screw of the

T-shape stick heads rests on the hat ring-arms, quasi-perpendicular to the sticks inclination (Fig. 3b). The hat base is hermetically closed by compressing the ring plus the plasticine against the soil surface. To this end, the screws are screwed against the T-shape iron arms welded on the hat ring. To prevent the stick turns-around itself, the external leg of the T-shape sticks should be rest on the soil surface (Fig. 3b). Once the HI base is installed, the bubble tower is connected to the HI air inlet tube (Fig. 3a) and the water-supply reservoir is assembled to the hat base. Next, the air flow plastic stopcock is opened, the water flow ball valve turned off, and the water reservoir filled with water. Finally, the pressure transducer is connected to the datalogger. Saturated infiltration measurements require that the pressure head inside the bubble tower is equal to the distance between the soil surface and the air outlet on the hat base (Fig. 1a). To start the infiltration measurements, the water flow ball valve is turned on and the air flow plastic stopcock is kept opened until the water level inside the hat reaches 2 to 4 cm height. This mechanism allows the air flows from the hat to the water reservoir as the hat is filling with water. Once the air flow plastic stopcock is closed, the air for water infiltration is immediately supplied from the bubble tower. Pressure head measured by the water manometer (h_M) corresponds to the pressure head supplied by bubble tower (h_{BT}) plus the distance between the hat-air inlet and the water level inside the hat (h_{WL}) (Fig. 3a).

The HI was validated in field conditions in an ungrazed field located in the Codo municipality (Moret-Fernández et al. 2011) by comparing the soil hydraulic properties estimated with HI with those measured with a M_{BD}. A total of eight soil infiltration measurements were completed. All infiltration measurements were taken on a nearly level area and on bared soil surfaces and ran up to 10 min. The pressure head applied on the soil surface was 0 cm. The *K* and sorptivity *S* at saturation were calculated using the new NSQE method (section 2.1).

3.- Results and discussion

3.1.- Estimate of K and S

The theoretical sensitivity of the NSQE method shows that accuracy to estimate the soil hydraulic properties depends on the infiltration time. Different *K* and *S* values within the interval of Eq.(5) were considered analyzing the minimum measurement time to obtain a given precision in the estimations. Two confidence intervals were studied, 10% and 90%, and an infiltrometer radius of 0.12m was considered (Fig. 4). Results show that small values of *K* and *S* require longer infiltration time if low errors are required.

As reported by Vandervaere et al. (2000), the water initially stored in the sand layer during the early stages of infiltration influences markedly the shape of cumulative infiltration curve (Fig. 2). This phenomena, which makes a jump in the firsts seconds of the cumulative infiltration curve, is more evident in the $\frac{dI}{d\sqrt{t}}$ vs. $\sqrt{t}$ relationship (Fig. 5.a.2) (Vandervaere et al., 2000). However, this method, which only allows a subjective approaching the time the wetting front needs to arrive to the soil surface (t_{sand}), turns practically unusable in noisy infiltration curves, where difficulties to detect t_{sand} increases (Fig. 5.2). These limitations vanished in the NSQE procedure, in which the infiltration steps corresponding to the sand layer are automatically omitted by looking for the best fitting between the experimental and the theoretical (Eq. 1) infiltration curves. On the other hand, the results show that NSQE method allowed a reasonable estimation of t_{sand} (Table 1). Once, the t_{sand} is estimated, the NSQE method satisfactorily fits the modelled vs experimental infiltration curves (independently on the contact sand layer) and calculates the *K* and *S* values (Fig. 5).

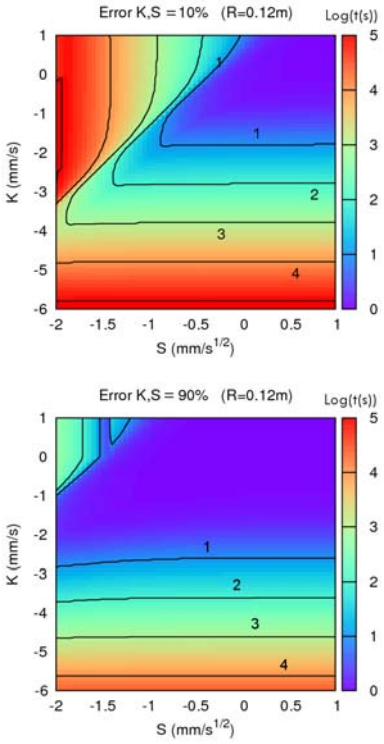

Figure 4. Required measurement time to obtain confidence intervals of 10% and 90% in the soil parameter estimation. An infiltrometer radius of 0.12m was considered in the calculations

Estimations of *K* and *S* values show that the DL method was only viable in no-noisy infiltration curves (Fig.5.b.2). In these cases, both DL and NSQE models gave comparable *K* and *S* values (Table 1). The large dispersion in the $\frac{dI}{d\sqrt{t}}$ vs. $\sqrt{t}$ relationship showed in the noisy curves (Fig. 5b.2) prevented to estimate realistic *K*, which may show erratic negative values (Table 2). This problem may be solved by decreasing the scanning time-

frequencies or removing undesirable points from the $\frac{dI}{d\sqrt{t}}$ vs. $\sqrt{t}$ plot. However, the subjectivity of this process, which depends on the researcher experience, makes the DL method to be, in many situations, subjective, inaccurate and unviable. These limitations were solved in the NSQE method, which demonstrated to be robust enough to calculate *K* and *S*, independently of the infiltration curve and the presence of contact sand layer.

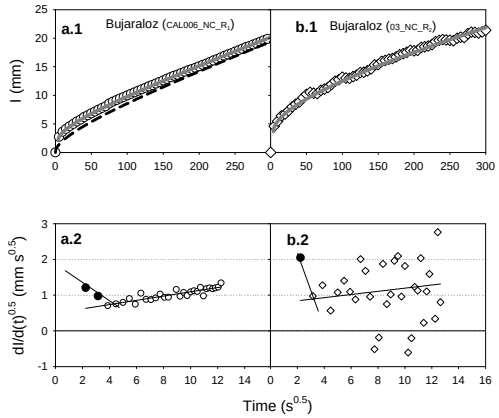

Figure 5. Comparison between cumulative infiltration curves measured (points) in two infiltration measurements in Bujaraloz, and the corresponding 3D modelled curves simulated from the hydraulic properties (Table 2) estimated with the differentiated linearization method (Eq. 5) (black discontinuous line) and the numerical solution of the 3D cumulative infiltration function (Eq. 1) (grey continuous line); and **a.2 to b.2**) the differentiated linearization method. Black points denote the section of the linear fitting curve corresponding to the contact sand layer and surface soil

Table 1. Soil sorptivity (S) and hydraulic conductivity (K) estimated with a 10 cm diameter disc infiltrometer in four different fields in Bujaraloz with the differentiated linearization (DL) and numerical solution of infiltration curve (NSQE) methods. RMSE and t_{sand} denotes the root mean square error and the time the wetting front need to cross the contact sand layer, respectively

Location	Field	DL			
		S ($mm\ s^{-05}$)	K ($mm\ s^{-1}$)	R^2	t_{sand} (s)
Bujaraloz	CAL006_NC_R1	0.51	0.0428	0.81	10-15
Bujaraloz	03_NC_R2	1.04	-0.0079	0.03	5-10
		NSQE			
		S ($mm\ s^{-05}$)	K ($mm\ s^{-1}$)	RMSE	t_{sand} (s)
Bujaraloz	CAL006_NC_R1	0.48	0.0393	0.091	4
Bujaraloz	03_NC_R2	0.69	0.0007	0.570	4

Over the 401 experimental infiltration measurements, only 131 curves (33%) could be analyzed by the DL method. From those, 112 curves had R^2 values between 0.15 and 0.60, and only 19 curves presented $R^2 > 0.6$. The infiltration curve noise, which significantly affects the $\frac{dI}{d\sqrt{t}}$ form (Fig. 5), was the main factor that prevented a good applicability of the DL method. Overall, the soil sorptivity estimated with the DL method was relatively well correlated to that calculated with NSQE model (Fig. 6). These results are due to the DL method is well defined in the early infiltration stages; where the capillary forces describing *S* dominates. The S_{DL} vs S_{NSQE} relationship for the $\frac{dI}{d\sqrt{t}}$ vs. $\sqrt{t}$ forms with $R^2 > 0.6$ was appreciably better that the corresponding values obtained for $R^2 < 0.6$ (Fig. 6).

A substantial worse K_{DL} vs K_{NSQE} correlation was observed. In this case, only $\frac{dI}{d\sqrt{t}}$ vs. $\sqrt{t}$ relationships with $R^2 > 0.7$ gave acceptable K_{DL} vs K_{NSQE} correlation (y = 0.982x - 0.004, $R^2 = 0.96$). For lower R^2 values, the DL method tended to overestimate *K*. Two reasons could explain these results: (i) small dispersion in $\frac{dI}{d\sqrt{t}}$ produces important changes the Eq.(2) slope, and consequently in K; in these cases only very accurate infiltration data can be used; and (ii) the short infiltration time allowed by the DL method (up to 150 s) prevented accurate estimation of K when slow infiltration rates are considered. As described in the section 3.1., short infiltration times from low soil conductive infiltration curves provide a wide incertitude to estimate *K*. This problem can be omitted by sampling longer infiltration measurements, for which only the NSQE method is viable.

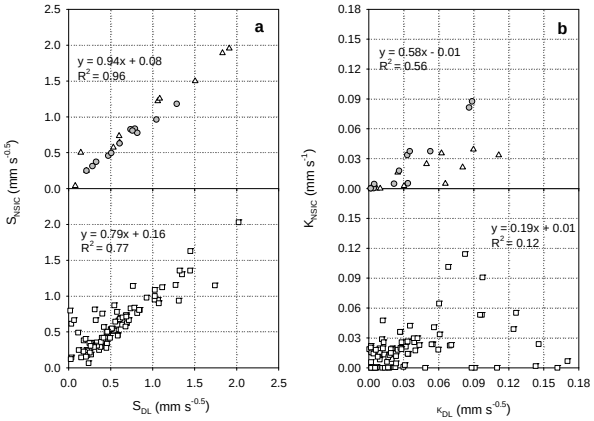

Figure 6. Relationship between the soil sorptivity (S) (a) and hydraulic conductivity (K) (b) estimated with the DL and NSQE models. Circles, triangles and squares points denote comparison between DL and NSQE methods for vs relationship with R^2 greater than 0.7, between 0.6 and 0.7 and between 0.2 and 0.6, respectively

3.2.- Disc base

Malleable disc base: The soil surface at the end of the infiltration measurement after removing the C_{DB} shows that the rigid base of the conventional disc cannot completely wet the soil surface when no sand contact layer is used (Fig. 7a). In contrast, both the C_{DB} with a sand contact layer and M_{DB} allow complete soil surface wetting even when non-smoothed soil surfaces are tested (Fig. 7b). These visual observations confirm that the M_{DB}

design may be a good alternative to the conventional disc. However, some care should taken when analysing these results because aggregate slaking/dispersion observed under the C_{DB} without contact sand (Fig. 7a) and the M_{DB} (Fig. 7c) may affect the infiltration rates and the calculated soil hydraulic properties. Soil aggregates may be less susceptible to slaking/dispersion if they were 'protected' from the disc infiltrometer membrane by a contact sand layer (Fig. 7b).

Comparison between the cumulative infiltration curves, *I(t)*, measured with C_{DB} and M_{DB} in a soil under NT tillage management allows the effect of the sand layer on the infiltration curve to be distinguished (Fig. 8). The *I(t)* curve obtained with C_{DB} shows a jump at the beginning of the experiment due to the contact sand layer. However, this jump vanishes in the M_{DB} *I(t)* curve, where the malleable disc base makes direct contact with the soil. Comparison between estimated *K* and *S* values in the different tillage treatments did not show significant differences between C_{DB} and M_{DB} (Table 2).

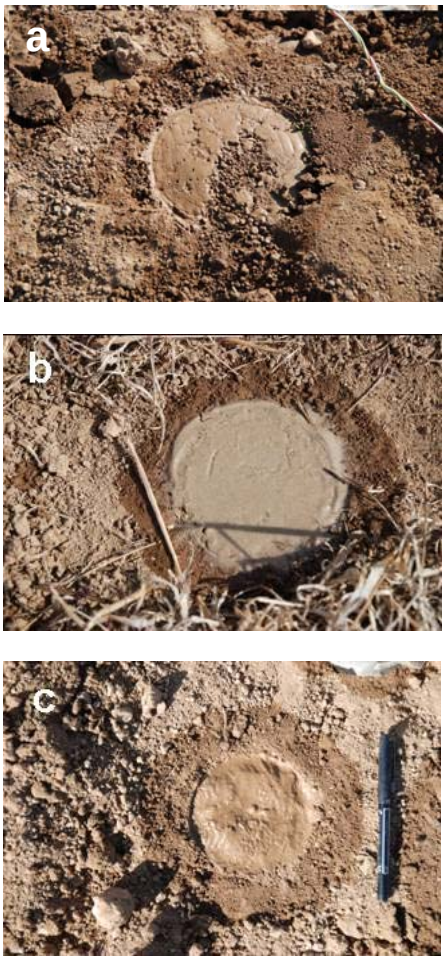

Fig 7. Soil surface at the end of an infiltration experiment after removing the conventional plate (a) without and (b) with a contact sand layer, and (c) after removing the malleable disc base

Hat infiltrometer: Field experiments showed that the three T-shape sticks plus plasticine system used to fix the hat infiltrometer on the soil surface resulted to be a portable and easy to install method, and hermetically close the base of the hat. The time needed to install the hat infiltrometer was less than 6 minutes. The system employed to fill up the hat with with a 2-4 cm height water sheet was 2-3 seconds. The lapse of time since the ball valve is open to the bubble tower starts to bubble was, on average, 5 seconds.

Table 2. *K* and *S* values calculated with the differentiated linearization (Eq. 8) applied to the C_{DB} and M_{DB} disc measurements on a loam soil under different tillage managements: conventional tillage (CT), reduced tillage (RT) and no tillage (NT)

Tillage	C_{DB}		M_{DB}	
	S (mm $s^{-0.5}$)	K (mm s^{-1})	S (mm $s^{-0.5}$)	K (mm s^{-1})
CT	1.30	0.026	0.86	0.036
RT	1.23	0.038	1.18	0.063
NT	0.46	0.013	0.41	0.013

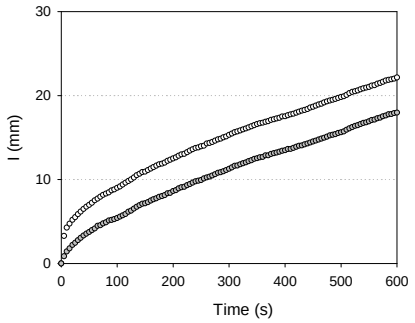

Fig 8. Cumulative infiltration curves on a soil under no-tillage treatments with the conventional (white circles) and malleable (grey circles) discs, respectively.

Cumulative infiltration curve obtained with HI showed a large jump in the firsts steps of the infiltration measurements (Fig. 9), that corresponds to the hat filling with a 2-4 cm height water sheet. This kind of cumulative infiltration curve can be easily analyzed by the numerical model described in section 2.1 (Fig. 9). The *K* and *S* values measured with the M_{DB} infiltrometer were within the same order of magnitude that those estimated with HI (Fig. 10). No significant differences ($p > 0.05$) were observed for the comparison between the *K* and *S* values estimated with M_{DB} and the corresponding values measured with HI.

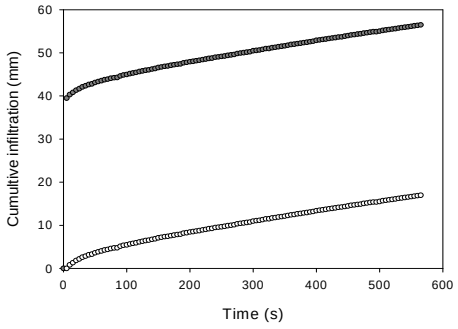

Fig 9. Original and corrected cumulative infiltration curves for a infiltration measurement performed on the landscape soil

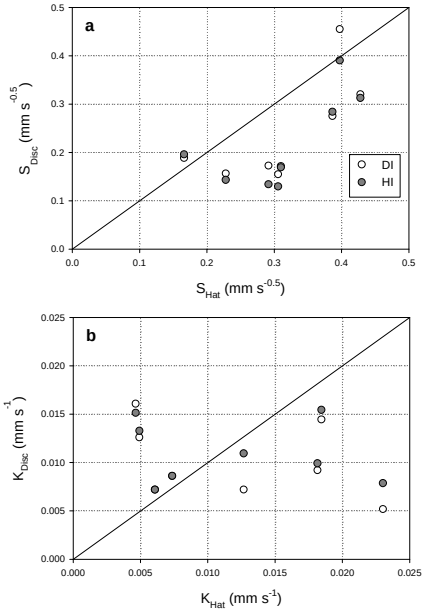

Fig 10. Comparison of sorptivity (S) and hydraulic conductivity (K) estimated with the hat (HI) and the disc infiltrometer (DI).

4.- Conclusions

This paper presents new advances to be applied to the disc infiltrometry technique: (i) a new method to estimate the soil hydraulic properties based on the quasi-exact equation of Haverkamp et al. (1994) for unsaturated cumulative infiltration; and (ii) new infiltrometer bases to measure the cumulative infiltration curve without contact sand layer. The theoretical sensitivity of the technique to estimate *S* and *K* was evaluated and compared to the corresponding simplified Haverkamp et al. (1994) equation. The analyzed infiltration measurements demonstrates that the proposed method allows satisfactorily estimate of the soil hydraulic properties independently on the data noise and the presence of contact sand layer. Although the DL model can give good approaches of *S*, even with noisy infiltration curves, this method demonstrates to be very inaccurate to estimate *K*. This limitation vanishes with the NSQE method, which is more robust, can work with longer infiltration times and allows better estimates of K and S. The new design of infiltrometer disc with a malleable membrane (M_{DB}) or the hat bases (HI), which allowed satisfactory estimated of the soil hydraulic properties without using a contact sand layer, can be promising alternatives to the conventional disc bases used in the infiltrometry technique. However, new experiments should be done to check the maximal soil tension supported by HI and the viability of these new designs in different soil types.

Acknowledgements. This research was supported by the Ministerio de Ciencia e Innovación of Spain (grant AGL2010-22050-C03-02) and by the Aragón regional government and La Caixa (Grants: GA-LC020/2010; GA-LC006/2008; 2012/ GA LC 074). The authors are grateful to Valero, Perez Ricardo Gracia, M. Josefa Salvador and Ana Bielsa for their help in various technical aspects of this study.

5.- References

Angulo-Jaramillo, R., J.P. Vandervaere, S. Roulier, J.L. Thony, J.P Gaudet, and M. Vauclin, 2000. Field measurement of soil surface hydraulic properties by disc and ring infiltrometers. A review and recent developments. *Soil Till. Res. 55*, 1–29.

Ankeny, M.D., M. Ahmed, T.C. Kaspar, and R. Horton, 1991. Simple field method determining unsaturated hydraulic conductivity. *Soil Sci. Soc. Am. J. 55*, 467– 470.

Casey, F.X.M., and N.E. Derby, 2002. Improved design for an automated tension infiltrometer. *Soil Sci. Soc. Am. J. 66*, 64–67.

Haverkamp, R., P.J. Ross, K.R.J. Smettem, and J.Y. Parlange, 1994. Three dimensional analysis of infiltration from the disc infiltrometer. Part 2. Physically based infiltration equation. *Water Resour. Res. 30*, 2931–2935.

Madsen MD, and D.G. Chandler, 2007. Automation and use of mini disk infiltrometers. *Soil Sci. Soc. Am. J. 71*, 1469–1472.

Minasny B, and A.B. McBratney, 2000. Estimation of sorptivity from discpermeameter measurements. *Geoderma 95*, 305–324.

Moret, D., J.L. and Arrúe, 2007. Dynamics of soil bulk properties during fallow as affected by tillage. *Soil Till. Res. 93*, 103-113.

Moret-Fernández, D., C. González-Cebollada, and B. Latorre, 2012a. New design of microflowmeter–tension disc infiltrometer: I. Measurement of the transient infiltration rate. *J. Hydrol. 466-467*, 151-158.

Moret-Fernández, D., B. Latorre, and C. González-Cebollada, 2012b. Microflowmetertension disc infiltrometer: Part II. Hydraulic properties estimation from transient infiltration rate analisis. *J. Hydrol. 466-467*, 159-166.

Moret, D., M.V. López, and J.L. Arrúe, 2004. TDR application for automated water level measurement from Mariotte reservoirs in tension disc infiltrometers. *J. Hydrol.* 297, 229-235

Moret-Fernández, D., G. Bueno, Y. Pueyo, and C.L. Alados, 2011. Hydro-physical responses of gypseous and non-gypseous soils to livestock grazing in a semi-arid region of NE Spain. *Agric. Water Manag. 98*, 1822-1827.

Moret-Fernández, D., C. Castañeda, E. Paracuellos, and J. Herrero, 2013. Hydro-physical characterization of contrasting soils in a semiarid zone of the Ebro river valley (NE Spain). *J. Hydrol.* In press.

Perroux, K.M., and I. White, 1988. Designs for disc permeameters. *Soil Sci. Soc. Am. J. 52*, 1205–1215.

Reynolds WD, 2006. Tension infiltrometer measurements implications of pressure head offset due to contact sand. *Vadose Zone J. 5*, 1287–1292.

Soil Survey Staff, 1975. Soil taxonomy: a basic system of soil classification for making and interpreting soil surveys. USDASCS Agric. Handbook 436. US Govt. Print. Office, Washington, DC.

Vandervaere, J.P., M. Vauclin, D.E. Elrick, 2000. Transient flow from tension infiltrometers. Part 1. The two-parameter equation. *Soil Sci. Soc. Am. J. 64*, 1263–1272.

Warrick, A.W., and P. Broadbridge, 1992. Sorptivity and macroscopic capillary length relationships. *Water Resour. Res. 28*, 427–431.

Warrick, A.W., and D.O. Lomen, 1976. Time-dependent linearized infiltration: III. Strip and disc sources. *Soil Sci. Soc. Am. J. 40*, 639–643.

Zhang, R., 1997. Determination of soil sorptivity and hydraulic conductivity from the disc infiltrometer. *Soil Sci. Soc. Am. J. 61*, 1024–1030.